Effect of frequency in the deposition of microcrystalline silicon from silane discharges

E. Amanatides, D. Mataras,[a] and D. E. Rapakoulias
Department of Chemical Engineering, Plasma Technology Laboratory, University of Patras, P.O. Box 1407, 26500 Patras, Greece

(Received 30 March 2001; accepted for publication 27 August 2001)

The influence of frequency in the range from 13.56 to 50 MHz, on the properties of 2% silane in hydrogen 0.5 Torr discharges used for the deposition of microcrystalline silicon thin films, has been investigated. The experiments were carried out under constant power conditions as determined through Fourier transform voltage and current measurements. The increase of frequency leads to a decrease of the rf field, an extension of the bulk, and a marked increase of the electron density and the amount of power consumed by electrons. These changes induce a decrease of the rate of high-energy electron–molecule collision processes (>10.5 eV) at higher frequencies and an enhancement of lower energy processes. Thus, there is a significant increase in the hydrogen flux toward surfaces, which can explain the beneficial effect of frequency to the crystallinity of μc-Si:H thin films. At the same time, SiH_4 electron impact dissociation is enhanced mainly due to the increase of electron density. On the contrary, ionization is not favored by the increase of frequency and the calculated ion flux toward the film surface indicates that the role of ions in a possible enhancement of the surface mobility of the film precursors is minor. The observed increase of the deposition rate is further discussed in terms of the nature of the film precursors and the spatial distribution of their production. © *2001 American Institute of Physics.*
[DOI: 10.1063/1.1413240]

I. INTRODUCTION

The use of hydrogenated microcrystalline silicon (μc-Si:H) as an intrinsic layer in thin film solar cells has been demonstrated to improve the stability of simple or tandem devices.[1] The most important drawback in this case is that the absorption coefficient of the material in the visible spectral region is low.[2] There are several ways to improve this situation among which the increase of the intrinsic layer thickness up to several microns is an inevitable one. However, the growth rate of μc-Si:H films deposited using highly diluted SiH_4 in H_2 discharges is generally not high enough to be acceptable in an industrial process.[3] Among other remedies, the increase of the driving frequency ($13.56\,\mathrm{MHz}<f<100\,\mathrm{MHz}$) has been proposed to be beneficial for the deposition rate,[4,5] as well as for the growth of microcrystals.[6] The observed increase of the growth rate was attributed to a boost of the radicals production rate due to an enhancement of the electron impact dissociation of SiH_4,[7,8] or alternatively to a higher surface reactivity due to an increase of the ion flux towards surfaces.[9] On the other hand, the reduction of the ion bombardment energy or the higher atomic hydrogen flux toward the growing film surface, were proposed for explaining the beneficial effect on the crystallinity of the film.[10] However, the above-mentioned explanations were based on previous studies concerning the effect of frequency on the gas phase and surface processes in pure SiH_4 and in SiH_4/H_2 discharges[7–9,11] used for the deposition of a-Si:H. Thus, besides the partially controversial explanations given, there are no studies specifically examining the influence of frequency on the properties of highly diluted SiH_4 in H_2 discharges that are commonly used for depositing μc-Si:H. This is attempted in the present work where the effect of frequency on the deposition process of μc-Si:H under constant power dissipation conditions is reported. This approach has been preferred against constant voltage or constant current conditions because it permits a more realistic comparison between the different frequency discharges while the effect of power under variable frequency operation is not well understood and is still under debate.[8] Thus, special attention has been given to the estimation of the power actually consumed in the discharge by applying an accurate method based on the Fourier transform of the voltage and current wave forms.[12] The proper combinations of the electrical parameters (voltage, current, and impedance) ensuring constant power dissipation at each frequency were then used in an analytical discharge model. The model considers the sheath dynamics as well as the mass transport of the charged particles in the bulk plasma,[13] aiming mainly at the prediction of the ion flux toward the surfaces and at the distinction of the fraction of power spend either for ion or for electron acceleration. Furthermore, the paths where electrons consume the fraction of the total power gained, are investigated by recording emission profiles of electronically excited species and by applying mass-spectrometric measurements of the total SiH_4 consumption in combination with a mass transfer model.[14]

[a]Author to whom correspondence should be addressed; electronic mail:dim@chemeng.upatras.gr

 © 2001 American Institute of Physics

Downloaded 06 Dec 2001 to 150.140.190.25. Redistribution subject to AIP license or copyright, see http://ojps.aip.org/japo/japcr.jsp

The results are discussed in terms of the changes in the ion flux, the silane dissociation rate, the role of hydrogen atoms, and the various film precursors.

II. EXPERIMENT

Film deposition studies have been performed in a capacitively coupled ultrahigh vacuum (UHV) parallel plate reactor having a base vacuum of 10^{-9} mbar. The reactor is equipped with a load lock system for the introduction of substrates and with four quartz windows suitable for spectroscopic observations. The 90 mm in diameter grounded (deposition) electrode is mounted on an UHV linear motion feedthrough, allowing continuous variation of the interelectrode space. In the present study the distance between the two electrodes was fixed at 1.7 cm. In all cases 2% SiH_4 in H_2 has been delivered in the reactor through a showerhead array of holes in the powered electrode, at a total pressure of 0.5 Torr. Pressure and flow rate were independently adjusted using a downstream throttle valve controller and upstream mass flow controllers, respectively. The films were deposited on Corning 7059 glass substrates heated at a temperature of 250 °C. The deposition rate was measured *in situ* using laser reflectance interferometry.

The measurements of the real power consumed in the discharge were based on Fourier transform voltage and current analysis. The excitation voltage and the discharge current signals were measured on the powered electrode lead, using a high impedance 1:100 attenuation voltage probe and an 0.1 Ω transfer impedance rf current probe. The method for the measurement of the power consumed in 13.56 MHz discharges and the extension to include higher frequencies have been presented in detail elsewhere.[13,15]

The setup used for recording emission intensities of SiH ($A\,^2\Delta \rightarrow X\,^2\Pi$) as well as α and β Balmer lines of atomic hydrogen, has been described in detail elsewhere.[16,17]

Mass spectrometric measurements have been performed using a Hidden analytical (HAL 301) quadrupole mass spectrometer connected at the exhaust port of the reactor. The gas sampled through a variable leak valve in a small chamber has been analyzed after 70 eV electron impact ionization. The partial pressure of H_2, SiH_4, Si_2H_6, and Si_3H_8 in the reactor was determined by measurements of the ion currents $I(m/e)$, at $m/e=2$, 32, 62, and 92, respectively, in order to minimize the contribution of higher homologus to the peaks measured.[18] The method used for the calibration and the transformation of SiH_4 and disilane partial pressures at the sample chamber to the correspondence partial pressures in the reactor were described in a previous work of this group.[19]

All the measurements reported here were performed in particle free conditions, as controlled by a laser light scattering technique.[20]

III. RESULTS AND DISCUSSION

A. Electrical measurements

Different sets of electrical measurements were initially performed in 0.5 Torr 2% SiH_4 in H_2 discharges at four distinct excitation frequencies (13.56, 30, 35, and 50 MHz), for finding the exact electrical conditions leading to constant

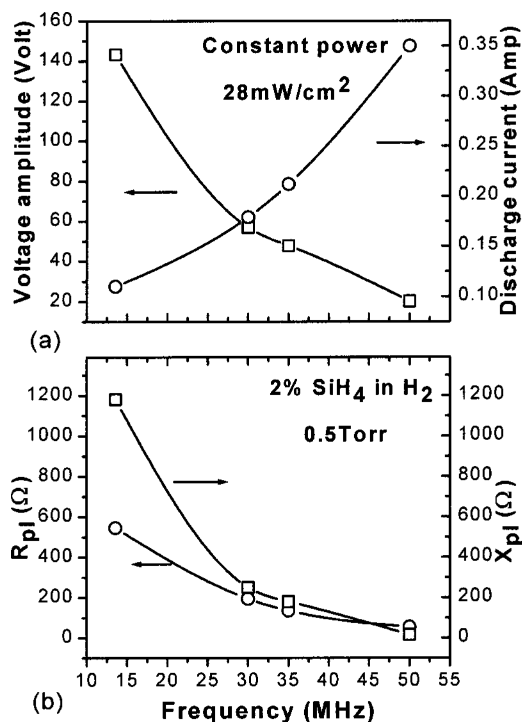

FIG. 1. The variation (a) of the total power dissipation and (b) of the power per discharge volume as a function of the electrode gap for 2% SiH_4 in H_2 discharges and frequencies of 13.56, 30, and 50 MHz.

power dissipation in the discharge. Thus, in Fig. 1(a) the measured values of voltage and current are plotted, ensuring a constant power consumption of 28 mW/cm^2 at each frequency, whereas Fig. 1(b) shows the reactive and resistive parts of the discharge impedance under the same conditions. As observed, a significant drop of the applied voltage [left axis, Fig. 1(a)] is required to counterbalance the large increase of the discharge current with frequency [right axis, Fig. 1(a)]. On the other hand, the discharge impedance decreases with increasing frequency and this is more pronounced up to 30 MHz for the reactive part X_{pl} [right axis, Fig. 1(b)] compared to the resistive part R_{pl} [left axis, Fig. 1(b)]. Previous work of this group concerning the variation of frequency in pure H_2 discharges[13] has shown that these changes induce major effects in most of the microscopic discharge parameters. More specifically, the spatial distribution of ions and electrons, the spatial distribution of the electric field, the plasma density, and the fraction of power spent for electrons and ions are all affected by the increase of frequency. In order to apply the same analysis in the present case as in the case of hydrogen, one must consider the implications resulting from the introduction of SiH_4 in the mixture.

Silane has a lower ionization threshold and a higher ionization cross section compared to H_2, while hydrogen ions H_x^+ ($x=1-3$) produced in the discharge undergo a very fast charge-transfer reaction with SiH_4, producing silicon hydride ions[21] (SiH_x^+). Thus, although SiH_4 concentration is rather low compared to H_2, SiH_x ions have to be considered in the analysis of ion transport in the sheaths and in the bulk. By taking into account only H_2^+ and SiH_3^+ ions for simplicity, the low field mobility of the i ion in the background gas j can be

Downloaded 06 Dec 2001 to 150.140.190.25. Redistribution subject to AIP license or copyright, see http://ojps.aip.org/japo/japcr.jsp

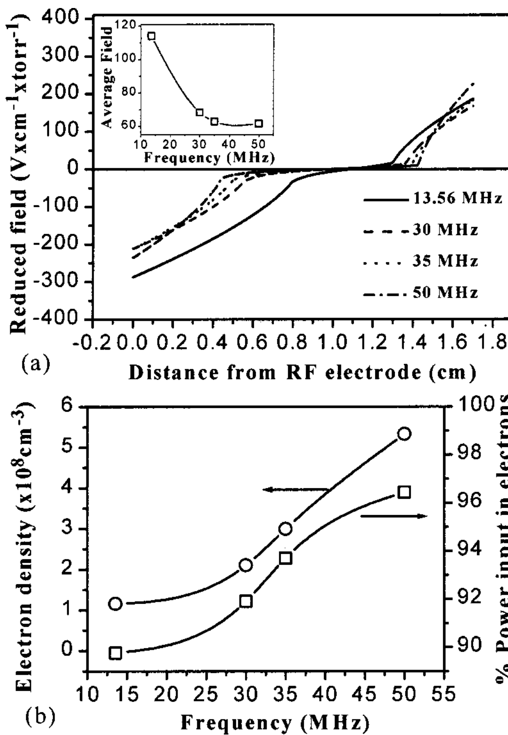

FIG. 2. (a) The total discharge current and (b) the phase of the discharge impedance φ_{el} as a function of the electrode gap and the discharge conditions of Fig. 1.

calculated according to the Langevin expression[22]

$$\mu_i P_j = 38.7 \times \left(\frac{m_j m_i}{m_j + m_i}\right)^{-1/2} \times T_{gas} \times \alpha_j^{-1/2}, \quad (1)$$

where α_j is the polarizability of gas j ($j = SiH_4, H_2$), m_j and m_i the masses of the neutral and ion species, respectively, T_{gas} the gas temperature, and P_j the partial pressure of j. The mass of ions m_i in the specific conditions was taken as the reduced mass of H_2^+ and SiH_3^+ ions.

On the other hand, the high field ionic mobility, required in the analysis of the transport in the sheaths, is estimated from the expression of the drift velocity[22]

$$\mu_{i,j} P = 10.73 \times \left(m_i \frac{m_j m_i}{m_j + m_i}\right)^{-1/4} \times \left(\frac{e}{Q}\right)^{1/2} (k_b T_{gas})^{-1/2} \left(\frac{E}{P_j}\right)^{-1/2}, \quad (2)$$

where $Q_{i,j}$ is the ion–molecule collision cross section and k_b the Boltzmann constant. The value of the effective ionic mobility in the SiH_4/H_2 mixture is then calculated using Blanc's law:

$$\frac{1}{\mu} = \frac{P_{SiH_4}/P_{TOT}}{\mu_{i,SiH_4}} + \frac{P_{H_2}/P_{TOT}}{\mu_{i,H_2}}. \quad (3)$$

With these considerations, one can apply the method used in Ref. 13 in the present experimental conditions. Thus, Fig. 2(a) presents the spatial distribution of the time-averaged electric field in the discharge. It is observed that as frequency increases the electric field is reduced and the low field bulk region is extended due to the decrease of the sheath lengths. The expansion of the bulk is followed by an increase of the electron density with frequency, the space-averaged value of which is presented in the left axis of Fig. 2(b). In addition, the lowering of the voltage required for maintaining constant power consumption as frequency increases [left axis, Fig. 1(a)] leads to a decrease of the power consumed for ion acceleration in the sheaths and consequently to an increase of the electron power [right axis, Fig. 2(b)]. In fact, the portion of power spent by electrons is very high (>88%) over the entire range of frequencies studied here and this is mainly a result of the low total power[23] (28 mW/cm^2).

The increase of the power consumed by electrons with frequency is very important because it has an immediate impact on the production of radicals through electron–molecule collisions; consequently, special attention must be paid to ensure the correctness of the model anticipation. In the present model the distinction between ion P_i and electron P_e power dissipation is based on the calculation of the ion power losses resulting from the ion conduction current and the voltage drop in both sheaths. This results in a relation of the form $P_i/P_e \propto \alpha(I/\omega^2)$, where I is the discharge current and α is a corrective factor accounting for the fact that ions injected in collisional sheaths have a velocity lower than Bohm's velocity. Godyak *et al.*[23] have initially applied this approach, which has been successfully compared to experimental measurements of the ion power dissipation, while other similar approaches concerning the issue can also be found in the literature.[24–26] Thus, Beneking[24] in an analysis of power dissipation in the sheaths and in the bulk has concluded in a relation of the form $P_i/P_e \propto \alpha(I^{3/2}/\omega^{5/2})$. Similarly, the analysis of Vahedi *et al.*[25] of the collisional heating case concludes in a relation of the form $P_i/P_e \propto V_{el}\omega^{1/2}$, where V_{el} is the applied electrode voltage, while Surenda and Graves[26] in their Monte Carlo simulation have predicted that the ratio of ion to electron power will scale as $P_i/P_e \propto I/\omega^2$. Application of all the above mentioned scaling laws in the present values of frequency, current, and voltage always leads to the same conclusion: The increase of frequency under constant total power conditions leads to an enhancement of the fraction of power dissipated in electrons.

In order to have an initial estimation of the electron–molecule collision processes that will be enhanced from the above-mentioned changes, a Boltzmann equation solver (written under the two-term approximation for the electron distribution function) has been used.[27] Thus, Fig. 3 presents the predicted % energy deposition in vibrational excitation, dissociation, electronic excitation, and ionization of H_2 and SiH_4 molecules as a function the reduced electric field for the 2% SiH_4 in H_2 mixture. Indices in Fig. 3 point out the space and time averaged values of the electric field [inset, Fig. 2(a)] at the different frequencies used here. A first important observation is that in such high dilution conditions almost 90% of the electron power is deposited in electron–H_2 collision processes for the entire range of the electric field values. Vibrational excitation and electronic excitation are the most energy consuming processes for low and high field values, respectively. Moreover, energy deposition in H_2 dissociation via the electron impact excitation of the $b\,^3\Sigma_u^+$

Downloaded 06 Dec 2001 to 150.140.190.25. Redistribution subject to AIP license or copyright, see http://ojps.aip.org/japo/japcr.jsp

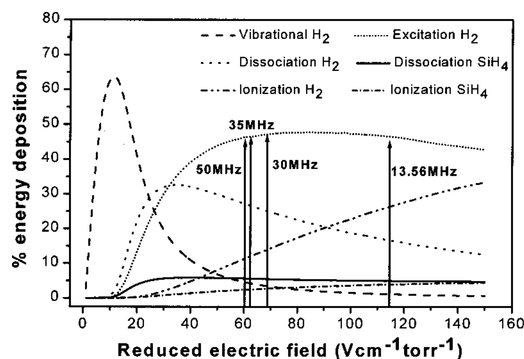

FIG. 3. (a) The % fraction of ion relative to electron power and (b) the variation of the self-bias potential as a function of electrode gap and the frequencies of 13.56, 30, and 50 MHz.

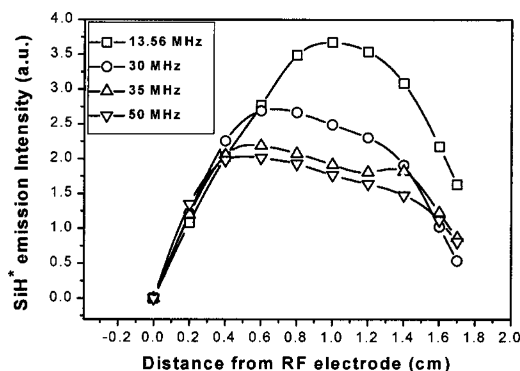

FIG. 4. The effect of the variation of electrode gap on: (a) the effective rate of momentum transfer though any type of electron collisions and (b) the ratio of bulk relative to sheath electron collisional heating at frequencies of 13.56, 30, and 50 MHz.

state,[28] a process of special importance in the deposition of μc-Si:H, presents a maximum at around 30 $\mathrm{V\,cm^{-1}\,Torr^{-1}}$ and then decreases with the increase of the field. This is due to the bell-shape type of the cross section for this process.[29] To the contrary, energy deposition in H_2 ionization increases very fast with the increase of the field and above 90 $\mathrm{V\,cm^{-1}\,Torr^{-1}}$ dominates over H_2 dissociation, even though these processes have a difference in their energy thresholds of about 7 eV.

Concerning energy deposition in electron–SiH_4 collisions processes, SiH_4 dissociation is the most energy-consuming process but due to the low fraction of SiH_4 in the gas mixture, it does not exceed 6% of the total. The fact that it remains almost constant over the entire range of field values is related to the cross section of this process that increases almost linearly with electron energy. Energy deposition in SiH_4 ionization, as in the case of H_2 ionization, increases rather fast with the field, however it becomes comparable to SiH_4 dissociation only for field values above 100 $\mathrm{V\,cm^{-1}\,Torr^{-1}}$.

Finally, taking into account the drop of the electric field necessary for maintaining constant power dissipation, as frequency increases [Fig. 2(a), indices in Fig. 3], a qualitative discussion of the redistribution of the electron energy deposition in collision processes with frequency can be made. Thus, electronic excitation of H_2 will consume about 50% of the electron power independent of frequency. However, H_2 dissociation is the process that is mostly enhanced by the increase of frequency as the % energy deposition for this process increases from 15% to 25%. This increase can have a major impact since hydrogen atoms are commonly assumed to have a significant role in the deposition process[30] of μc-Si:H. Furthermore, at 13.56 MHz, due to the quite higher electric field value, H_2 ionization is the favored process by consuming 25% of the electron power, while the increase of frequency leads to a monotonic decrease of the fraction of power consumed for it. In addition, by examining the ionization processes for both gases in the mixture one can say that the increase of frequency will enhance SiH_4 ionization relative to H_2 ionization. Concerning SiH_4 dissociation, the almost constant energy deposition over the entire range of field values leads to the conclusion that the increase of frequency will enhance this process only due to the increase of the total power dissipated by electrons [Fig. 2(b), right axis]. The weight of both these factors in an increase of SiH_4 electron-induced dissociation with frequency will be further discussed later in conjunction with results concerning silane consumption in the discharge.

The accuracy of the qualitative discussion presented above can be affected by the fact that Boltzmann solution using the two-term expansion is less accurate for gases in which a vibrational cross section maximum overlaps a Ramsauer minimum of the momentum transfer cross section[31] and this is the case for SiH_4. In addition, superelastic collisions have also been found to affect the electron energy distribution function shape in the case of H_2 and H_2 rich discharges[32] and this type of collision is not included in the solver used in this study. For this purpose, the discussion has been limited to qualitative predictions, instead of presenting the electron–molecule collision rates predicted by the Boltzmann solver. The best way to confirm the above predictions is by a comparison with experimental observations concerning the effect of frequency on high-energy processes as will be attempted in the following section.

B. Electron–molecule collision processes

1. Dissociative excitation

Spatially resolved optical emission spectroscopic measurements of SiH ($A\,^2\Delta$), as well as of α and β Balmer lines of atomic hydrogen, were performed at different frequencies and under the conditions of constant power dissipation. Figure 4 presents the time-averaged axial emission profiles resulting from one-electron impact dissociative excitation of SiH_4 towards SiH ($A\,^2\Delta$), the process threshold being 10.5 eV. As observed, the increase of frequency is followed by a reduction of the effective electron population for the specific process, which is again more pronounced between 13.56 and 30 MHz, and by an alteration of the intensity distribution in the interelectrode space. The change in the spatial profile is determined mainly by the decrease of the powered electrode sheath length with frequency. Namely, at 13.56 MHz the wide sheath of the powered electrode leads to a profile that is displaced toward the grounded electrode

Downloaded 06 Dec 2001 to 150.140.190.25. Redistribution subject to AIP license or copyright, see http://ojps.aip.org/japo/japcr.jsp

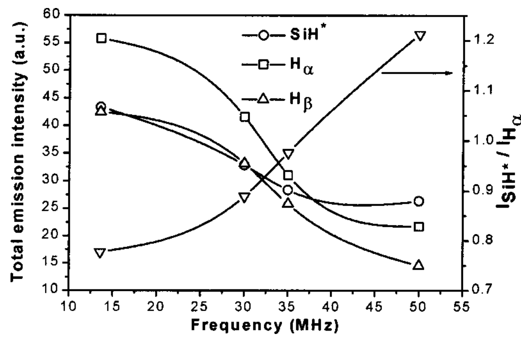

FIG. 5. The spatial distribution of the SiH ($A\ ^2\Delta$) emission intensity at five different electrode gaps and (a) the frequency of 50 MHz and (b) the frequency of 30 MHz.

while the increase of frequency induces a displacement of the maximum rate of production toward the rf electrode.

The reduction of the high-energy electron population with frequency that results in the observed drop of SiH ($A\ ^2\Delta$) emission intensity is also present in emission measurements of the α and β Balmer lines of atomic hydrogen. Both processes in highly diluted SiH_4 in H_2 discharges have been proven to originate from one electron impact dissociative excitation[33] of H_2. The energy thresholds of these processes (16.6 and 17.5 eV, respectively) are quite large, while their cross sections are more than 1 order of magnitude smaller, compared to SiH_4 dissociative excitation. Thus, it is not surprising that the total production of the SiH ($A\ ^2\Delta$) radical, as calculated by integrating the emission profiles in space (Fig. 5), is comparable to the production of excited hydrogen atoms, although SiH_4 concentration is much smaller than H_2. As observed in Fig. 5 the total production rate of all the species decreases with frequency, however in a different manner for each species, resulting to a higher production rate for SiH ($A\ ^2\Delta$) compared to excited hydrogen atoms at 50 MHz. Thus, one can say that the increase of frequency under constant power conditions leads to a decrease of the rate of high-energy electron–molecule collision processes, with this reduction being more pronounced for processes with higher energy thresholds.

Furthermore, emission measurements can also be used to estimate the effect of frequency on SiH_4 and H_2 ionization; processes with increased importance due to their strong dependence on frequency.

2. Ionization

Ions in the SiH_4/H_2 discharge originate from electron impact dissociative ionization of either SiH_4 or hydrogen:

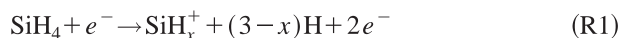

$$SiH_4 + e^- \rightarrow SiH_x^+ + (3-x)H + 2e^- \qquad (R1)$$

$$H_2 + e^- \rightarrow H_2^+ + 2e^-. \qquad (R2)$$

Considering the small difference between the energy thresholds of excitation and ionization in SiH_4(11.8–10.5 eV) and H_2(15.5–16.6 eV), it is expected that the increase of frequency under constant power dissipation will lead to a drop of both hydrogen and silane ionization rates. In this sense, one can express the ionization rate constants as functions of the excitation rate constants

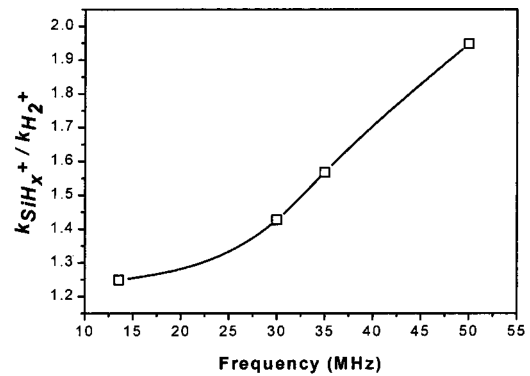

FIG. 6. (a) The total SiH ($A\ ^2\Delta$) intensity and (b) the space average SiH ($A\ ^2\Delta$) intensity as a function of the electrode gap at two frequencies of 30 and 50 MHz.

$$k_{SiH_x^+} = \frac{Q_{SiH_x^+}}{Q_{SiH(A\,^2\Delta)}} k_{SiH(A\,^2\Delta)}$$

and

$$k_{H_2^+} = \frac{Q_{H_2^+}}{Q_{H_\alpha}} k_{H_\alpha}, \qquad (4)$$

where $Q_{SiH_x^+}$, $Q_{SiH(A\,^2\Delta)}$, $Q_{H_2^+}$, and Q_{H_a} are the cross sections for the specific processes.[34–36]

Moreover, the ratio of SiH ($A\ ^2\Delta$) to H_α total emission intensity plotted in the right axis of Fig. 5 can be expressed as

$$\frac{I_{SiH(A^2\Delta)}}{I_{H_\alpha}} = \frac{\bar{k}_{SiH(A\,^2\Delta)}\bar{n}_e[SiH_4]d}{\bar{k}_{H_a}\bar{n}_e[H_2]d}, \qquad (5)$$

where $\bar{k}_{SiH(A\,^2\Delta)}$, $\bar{k}_{H_a}$ are the space averaged rates of SiH_4 and H_2 dissociative excitation to SiH($A\ ^2\Delta$) and H_α, respectively, $\bar{n}_e$ the space averaged electron density, d the electrode gap, and $[SiH_4]$, $[H_2]$ the concentrations of silane and hydrogen in molecules/cm^3.

A combination of Eqs. (4) and (5) results in an expression that relates SiH_4 and H_2 ionization rate constants

$$\frac{k_{SiH_x^+}}{k_{H_2^+}} = \left(\frac{I_{SiH(A\,^2\Delta)}}{I_{H_a}}\right)\left(\frac{Q_{SiH_x^+}}{Q_{SiH(A\,^2\Delta)}}\right)\left(\frac{Q_{H_a}}{Q_{H_2^+}}\right)\frac{[H_2]}{[SiH_4]}. \qquad (6)$$

The variation of this ratio with frequency is plotted in Fig. 6 showing that the increase of frequency leads to an enhancement of the ionization rate of SiH_4 relative to H_2. This result is in very good agreement with the Boltzmann solution (Fig. 3), which predicts a very fast drop of the energy consumed for H_2 ionization and an enhancement of the energy dissipation in SiH_4 ionization relative to H_2 with increasing frequency.

Downloaded 06 Dec 2001 to 150.140.190.25. Redistribution subject to AIP license or copyright, see http://ojps.aip.org/japo/japcr.jsp

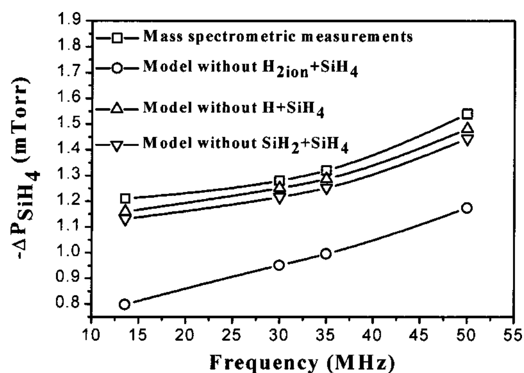

FIG. 7. The variation of the deposition rate (left axis) and of the total silane consumption (right axis) as a function of the electrode gap for the 30 MHz excitation.

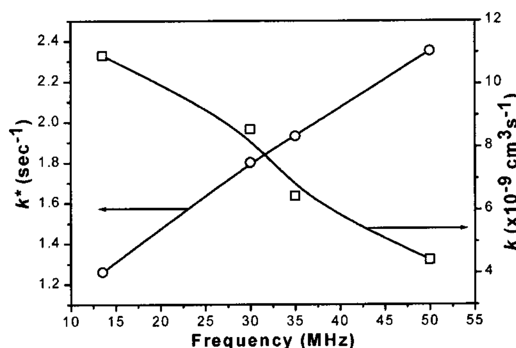

FIG. 8. The variation of the deposition rate (left axis) and of the total silane consumption (right axis) as a function of the electrode gap for the 50 MHz excitation.

3. SiH_4 *dissociation*

The mass-spectrometric measurements of the total SiH_4 conversion in the reactor, performed under the same conditions, are presented in Fig. 7. SiH_4 conversion remains rather low (<16%) over the entire range of frequencies due to the low total power consumption, while there is a slight increase of SiH_4 consumption when increasing frequency from 13.56 to 35 MHz that is more pronounced at 50 MHz.

The main reactions that are expected to consume SiH_4 in the case of highly diluted SiH_4 in H_2 discharges are[14]

$$e^- + SiH_4 \rightarrow SiH_x + (4-x)H \quad (x=0-3), \tag{R3}$$

$$H_2^+ + SiH_4 \rightarrow SiH_3^+ + H_2 + H, \tag{R4}$$

$$H + SiH_4 \rightarrow SiH_3 + H_2, \tag{R5}$$

$$SiH_2 + SiH_4 \rightarrow Si_2H_6. \tag{R6}$$

A mass transfer model, described in detail in Ref. 14, was used to distinguish SiH_4 consumption due to electron impact dissociation (R3) from the consumption in reactions with ions or radicals [(R4) (5), (6)]. Briefly, the model simulates SiH_4/H_2 discharges in a parallel plate reactor, involving gas phase kinetics, mass transfer, and surface chemistry. The required inputs are the total SiH_4 consumption and the spatial distribution of silane electron induced dissociation that in this case is taken from the spatial laser induced fluorescence measurements of the ground state $SiH(X\,^2\Pi)$ radical.[14]

Application of the model to the present experimental conditions permits the calculation of the rate of production of effective electron population for SiH_4 dissociation ($k^* = k\bar{n}_e$), presented in Fig. 8. As shown, k^* increases linearly with frequency, varying from 1.25 s^{-1} at 13.56 MHz to 2.3 s^{-1} at 50 MHz. However, if one separates the dependence of k^* on the rate constant k from the influence of the average electron density $\bar{n}_e$ the result is that the observed linear increase can be attributed to the competitive increase of the electron density [Fig. 2(b), left axis] along with the drop of the electron energy dependent rate constant k (Fig. 8, right axis).

The predicted dependence of the dissociation rate of SiH_4 on frequency is similar to that presented from Sansonnens *et al.*[8] although that work concerned pure SiH_4 discharges while a different technique was used for the calculation of SiH_4 depletion in the discharge. The increase of the dissociation rate predicted by the model is also in agreement with the results of the Boltzmann solution presented above, where an enhancement of SiH_4 dissociation caused by the increase of the fraction of power dissipated by electrons was anticipated. The increase of the electron power was attributed to the increase of electron density, which as explained above, causes an increase of the effective electron population for silane dissociation.

The different trends of the dissociation rate and the consumption of SiH_4 with frequency that can be observed by comparing Figs. 7 to 8 reveal the relative contribution of reaction (R3), and Eqs. (4), (5), and (6) to the total SiH_4 consumption. The specific weight of these reactions has been checked by successively excluding reactions (R4), (R5) and (R6) from the mass transfer model, while using in all cases the value of the electron impact dissociation rate of SiH_4 calculated by the model with the complete set of reactions (Fig. 7). It can be observed that reactions (R5) and (R6) have only a minor influence at all frequencies, their exclusion leading to an underestimation of less than 8% of the experimentally measured conversion of SiH_4. On the other hand, reaction (R4) appears to be much more important, being responsible for about 35% of SiH_4 consumption at 13.56 MHz, whereas the increase of frequency leads to a reduction to no less than ~25%. The differentiation of the importance of reaction (R4) between 13.56 MHz and the other frequencies is related to the enhancement of H_2 ions production at 13.56 MHz (Figs. 3 and 6). Thus, the existence of this significant consumption path at 13.56 MHz is responsible for the abovementioned different trends between SiH_4 consumption and electron induced dissociation rate with frequency.

To summarize the results of the mass spectrometric measurements and the mass transfer model, the increase of frequency under constant power conditions was found to enhance the electron impact dissociation rate of SiH_4 mainly through the increase of electron density. In the frequency range from 30 to 50 MHz, electron impact dissociation to neutral radicals is responsible for about 70% of total SiH_4 consumption. At 13.56 MHz due to an increase of the relative importance of SiH_4 reaction with H_2 ions, the contribution of SiH_4 dissociation rate to the total SiH_4 consumption

Downloaded 06 Dec 2001 to 150.140.190.25. Redistribution subject to AIP license or copyright, see http://ojps.aip.org/japo/japcr.jsp

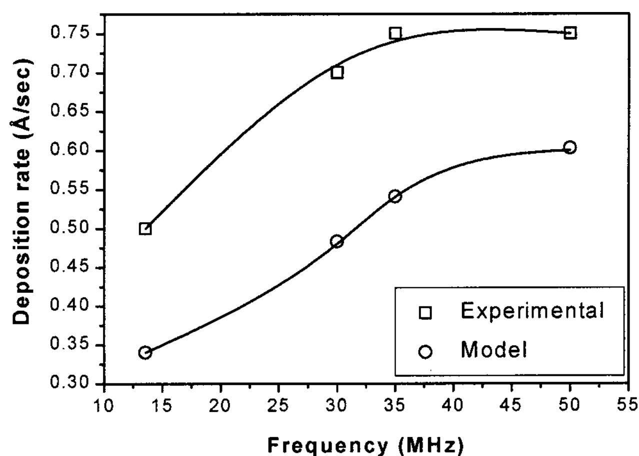

FIG. 9. Experimentally measured and model predicted film growth rates as a function of frequency.

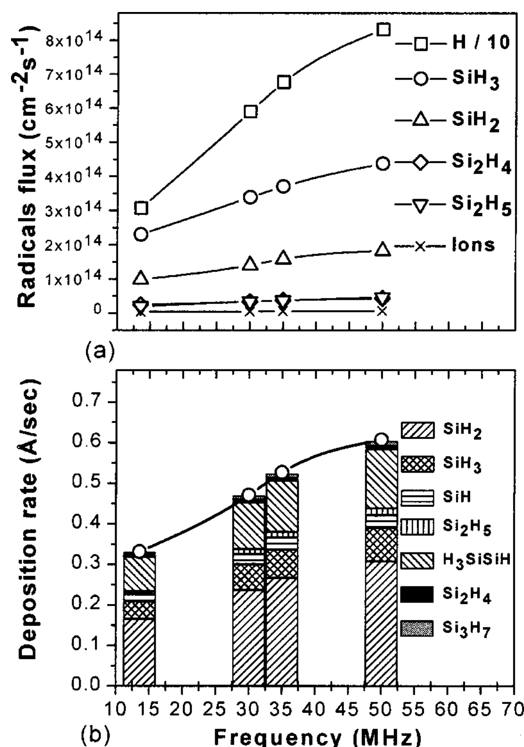

FIG. 10. (a) Radicals, atomic hydrogen, and ions fluxes as a function of frequency and (b) the contribution of the main radicals to the calculated values of the deposition rate at different frequencies.

drops to ~60%. This difference is expected to induce changes in the composition of the flux reaching the growing surface, thus affecting the film growth rate.

C. Deposition rate measurements

The variation of the film growth rate with frequency is presented in Fig. 9. The deposition rate under these very high dilution and rather low power conditions is low while the film crystallinity is around[37] 70%. The deposition rate increases linearly with frequency up to 35 MHz and then remains almost constant up to 50 MHz. Thus, the trend of the deposition rate with frequency is not similar to either SiH_4 consumption (Fig. 7) or SiH_4 dissociation rate (Fig. 8). In fact, the enhancement of the deposition rate is more pronounced when increasing frequency from 13.56 to 35 MHz (50%) where the respective increase of SiH_4 consumption is less than 10%. Moreover, the increase of the dissociation rate by 55% when going from 13.56 to 35 MHz (Fig. 8, left axis) can explain the 50% increase of the deposition rate, however it fails to explain the observed constant deposition rate between 35 and 50 MHz.

The disagreement between the trends discussed above leads to the conclusion that the deposition rate depends drastically on other parameters like the radicals sticking coefficients, the hydrogen atoms/ions flux toward the surface, and the spatial distribution of the dissociation rate. The results of the mass-transfer model present an effort to include these factors in the prediction of the deposition rate. As shown in Fig. 9, the model underestimates the deposition rate by ~30% due to the choice of a rather conservative set of sticking coefficients. In addition, the ion core model[38] that has been adopted for the branching ratio of SiH_4 dissociation is most probably underestimating the production of highly sticking SiH_2 radicals, contributing also in the deviation of the calculated values of the deposition rate from the experimental ones. However, the model can very well reproduce the experimentally measured increase of about 50% between 13.56 and 35 MHz and the tendency for constant film growth rate with a further increase.

This allows for a discussion of the effect of frequency on the relative contribution of the radicals to the film growth. Thus, Fig. 10(a) presents the radicals/ions fluxes toward the grounded electrode as predicted by the model, corresponding to the calculated values of the deposition rate (Fig. 9). The flux of hydrogen atoms dominates by far silicon hydride and ion fluxes over the entire range of frequencies, while it is almost tripled when increasing frequency from 13.56 to 50 MHz. The enhancement of H_2 dissociation to hydrogen atoms with frequency has been predicted in the analysis of the fraction of the power spent for electron–molecule collision processes (Fig. 3). This increase is reflected on the flux of hydrogen atoms, since under these conditions diffusion dominates over reaction (R5), the main reaction that can consume atomic hydrogen before reaching the surfaces.

Despite the significantly high flux of hydrogen atoms, the calculated etch rate is negligible as the relative probability of–SiH_3 etching (P_{etch}) and–H abstraction P_{ab} from the growing surface is quite low. Abrefah and Olander[39] have proposed a relation of silicium etching versus H abstraction that at the present experimental conditions ($T_{sub}=500\,K$) leads to a ratio of $P_{etch}/P_{ab}=0.06$ and to etch rates less than 1% of the deposition rate. Srinivasan and Parson[40] have estimated a higher ratio ($P_{etch}/P_{ab}\sim 0.2$), however even in this case the etch rates remain lower than 10% of the total deposition rate.

The main effect of this high H flux consists of local heating of the growth surface and subsurface, affecting the surface mobility of the film precursors and enhancing the formation of microcrystals.[41] Taking into account that the ion flux (Fig. 10) is about 2 orders of magnitude less than H atoms one can say that the increase of the hydrogen atoms flux with frequency is the main reason explaining the obser-

Downloaded 06 Dec 2001 to 150.140.190.25. Redistribution subject to AIP license or copyright, see http://ojps.aip.org/japo/japcr.jsp

vation that higher frequencies favor μc-Si:H formation.[6]

Concerning the flux of silicon hydrides, the increase of frequency leads to a continuous increase of all radicals reaching the surface [Fig. 10(a)]. Silyl radical (SiH_3) dominates over all other silicon containing species being ~2.5 times higher than silylene (SiH_2) and about 1 order of magnitude higher than silicon oligomers (Si_2H_5, $H_2Si{=}SiH_2$, and H_3SiSiH). This is due to the lower gas-phase reactivity of SiH_3 compared to SiH_2, whereas the production of Si_2H_2 and Si_2H_4 from secondary gas phase reactions is not favored under the present conditions.[14]

In Fig. 10(b), is presented the contribution of the main radicals to the film growth. It is observed that despite the high SiH_3 flux, the contribution of this radical [Fig. 10(b)] to the calculated values of the deposition rate is only about 20%, while SiH_2 contributes by more than 50%. This is a result of the quite different sticking probabilities s of these radicals[42–44] (0.09 and 0.65, respectively). The abovementioned increase of the hydrogen flux with frequency can also affect the sticking probability of the SiH_3 radical by reducing its effective residence time in the physisorpted state.[43] This will normally lead to a further reduction of the sticking coefficient and consequently the contribution of the radical in the film growth. Therefore, it appears that the increase of frequency will lead to an enhancement of the contribution of SiH_2 to the film growth relative to SiH_3. However, other factors like the gas phase reactivity of SiH_2 and the spatial distribution of silane dissociation have to also be considered in order to understand the observed effect of frequency on the film growth rate. The SiH_2 radical is created through electron-impact dissociation of SiH_4 and consumed by gas phase reaction with SiH_4 and diffusion to the walls, the rate constant of the reaction of SiH_2 with H_2 being rather low[45] ($5\times10^{-14}\,cm^3/s$). Consequently, the diffusion length Λ of SiH_2 wherever it is produced in the discharge is given by the ratio

$$\Lambda=\sqrt{\frac{D_{SiH_2}}{k_{SiH_2+SiH_4}[SiH_4]}},$$

where D_{SiH_2} is the diffusion coefficient of SiH_2 in the SiH_4/H_2 mixture and $k_{SiH_2+SiH_4}$ is the rate constant of the SiH_2+SiH_4 reaction. In the present conditions Λ takes the value of 0.5 cm, meaning that the fraction of SiH_2 that is lost in the grounded electrode contributing to the film growth will be strongly determined by the spatial distribution of SiH_4 dissociation. Thus, the displacement of SiH_4 dissociation far for the grounded electrode will enhance SiH_2 consumption in the gas phase instead of loss in the surface. The increase of frequency displaces the maximum of the radicals production far from the grounded electrode, due to the decrease of the sheath width of the powered electrode (Fig. 4). This seems to be the main reason for the observation that the increase of SiH_4 dissociation rate by 30% between 30 and 50 MHz (Fig. 8) is followed by a slight increase of the deposition rate by only 7% (Fig. 9). This aspect is further supported by a previous work of this group[46] where the investigation of the effect of the variation of the interelectrode gap on the μc-Si:H deposition rate from 30 and 50 MHz 2% SiH_4 in H_2 discharges has been reported. The optimum of the interelectrode gap has been found to shift from 1.5 to 1.3 cm as frequency increases.

Finally, the increase of frequency shows a rationalistic way to enhance SiH_4 and H_2 dissociation rates through low electric fields and high electron densities. However, this is not the only way to increase the film growth rate or to ensure conditions of low electric field and high electron density. The combination of 13.56 MHz and very high pressure[47] (>3 Torr) or 30 MHz, 1 Torr highly diluted SiH_4 in H_2 discharges[48] have also been used to obtain very high μc-Si:H deposition rates.

IV. CONCLUSIONS

The effect of radio frequency (13.56–50 MHz) under conditions of constant power dissipation on the properties of highly diluted SiH_4 in H_2 discharges used for depositing μc-Si:H thin films has been reported. A combination of electrical, emission, mass spectrometric, and deposition rate measurements together with a model of plasma physics and a mass transfer model have been applied to reveal the basic characteristics of these discharges.

As frequency increases, the constant power dissipation induces a drop of the electric field, an increase of the electron density, and an enhancement of the power consumed by electrons. These changes lead to a decrease of the rate of the high-energy electron–molecule collision processes (>10.5 eV) at higher frequencies, the reduction being more pronounced for processes with higher energy threshold. Thus, hydrogen dissociation is favored by the increase of frequency leading to a significant increase of the hydrogen flux toward the surfaces. This enhancement is estimated to be the main reason behind the observation that higher frequencies favor the growth of μc-Si:H thin films. At the same time, SiH_4 electron impact dissociation is also enhanced by the increase of frequency due mainly to the higher electron density.

The increase of the deposition rate with frequency is not solely related to the increase of the dissociation rate of SiH_4. As the highly sticking, highly reactive SiH_2 radical is found to be the main film precursor and the diffusion length of this radical is smaller than the interelectrode gap, the film growth rate is very sensitive on the spatial distribution of the source of these radicals. The displacement of the maximum rate of radical production toward the rf electrode leads to a weakening of the dependence of the deposition rate on the SiH_4 dissociation rate.

The ion flux toward the film surface has been found to be about 1 order of magnitude less than that of neutral radicals and about 2 orders of magnitude less than the flux of hydrogen atoms, thus their importance in the film growth or in a possible enhancement of the surface mobility of film precursors is minor.

Finally, the increase of frequency is a measure that can lead to the increase of SiH_4 and H_2 dissociation through low electric fields, an increase of the power transferred to electrons, and higher electron densities. These conditions are generally considered beneficial for the film growth while re-

Downloaded 06 Dec 2001 to 150.140.190.25. Redistribution subject to AIP license or copyright, see http://ojps.aip.org/japo/japcr.jsp

ducing the possibility of particles formation, however they can also be fulfilled by adjusting other macroscopic discharge parameters as the total pressure and the power. An increase of the fraction of SiH_4 in the gas mixture is also required in order to have a more rationalistic consumption of the electron power in electron–SiH_4 collisions, while the diffusion length of highly sticking radicals relative to the interelectrode gap has to also be considered.

[1] N. Wyrch *et al.*, Proceedings of the 2nd World Conference on Photovoltaic Energy Conversion, Vienna, 1998, Vol. I, pp. 467–471.
[2] J. Meier, R. Fluckiger, H. Keppner, and A. Shah, Appl. Phys. Lett. **65**, 860 (1994).
[3] M. Tzolov, F. Finger, R. Carius, and P. Hapke, J. Appl. Phys. **81**, 7376 (1997).
[4] P. Torres, H. Keppner, J. Meier, U. Kroll, N. Beck, and A. Shah, Physica Status Solidi **97–039**, R9 (1997).
[5] H. Curtins, N. Wyrsch, and A. Shah, Electron. Lett. **23**, 228 (1987).
[6] F. Finger, R. Carius, P. Hapke, L. Houben, M. Luysberg, and M. Tzolov, Mater. Res. Soc. Symp. Proc. **452**, 725 (1997).
[7] A. A. Howling, J.-L. Dorier, Ch. Hollenstein, U. Kroll, and F. Finger, J. Vac. Sci. Technol. A **10**, 1080 (1992).
[8] L. Sansonnens, A. A. Howling, and Ch. Hollenstein, Plasma Sources Sci. Technol. **7**, 114 (1998).
[9] M. Heintze, R. Zedlitz, and G. H. Bauer, J. Phys. D **26**, 1781 (1993).
[10] R. Fluckiger, J. Meier, M. Goetz, and A. Shah, J. Appl. Phys. **77**, 712 (1995).
[11] M. Heintze and R. Zedlitz, J. Non-Cryst. Solids **198**, 1038 (1996).
[12] N. Spiliopoulos, D. Mataras, and D. E. Rapakoulias, J. Vac. Sci. Technol. A **14**, 2757 (1996).
[13] E. Amanatides and D. Mataras, J. Appl. Phys. **89**, 1556 (2001).
[14] E. Amanatides, S. Stamou, and D. Mataras, J. Appl. Phys. **90**, 5786 (2001).
[15] N. Spiliopoulos, D. Mataras, and D. E. Rapakoulias, J. Vac. Sci. Technol. A **14**, 2757 (1996).
[16] D. Mataras, S. Cavadias, and D. E. Rapakoulias, J. Appl. Phys. **66**, 119 (1989).
[17] S. Stamou, E. Amanatides, D. Mataras, and D. E. Rapakoulias, Proceedings of 14th European Photovoltaic Solar Energy Conference, Barcelona, 1997, p. 664.
[18] P. A. Longeway, H. A. Weakliem, and R. D. Estes, J. Appl. Phys. **57**, 5499 (1985).
[19] N. Spiliopoulos, D. Mataras, and D. Rapakoulias, J. Electrochem. Soc. **144**, 634 (1997).
[20] S. Stamou, D. Mataras, and D. E. Rapakoulias, Chem. Phys. **218**, 57 (1997).
[21] W. N. Allen, T. M. H. Cheng, and F. W. Lampe, J. Chem. Phys. **66**, 3371 (1977).
[22] E. W. McDaniel and E. A. Mason, *The Mobility and Diffusion of Ions in Gases* (Wiley, New York, 1973).
[23] V. A. Godyak, R. B. Piejak, and B. M. Alexandrovich, J. Appl. Phys. **69**, 3455 (1991).
[24] C. Beneking, J. Appl. Phys. **68**, 4461 (1991).
[25] V. Vahedi, C. K. Birdsall, M. A. Lieberman, G. DiPeso, and T. D. Rognlien, Phys. Fluids B **5**, 2719 (1993).
[26] M. Surenda and D. B. Graves, Appl. Phys. Lett. **59**, 2091 (1991).
[27] BOLSIG (Shareware), Kinema Software (web site: http://www.csn.net/siglo).
[28] K. Hassouni, A. Gicquel, M. Capitelli, and J. Loureiro, Plasma Sources Sci. Technol. **8**, 494 (1999).
[29] H. Tawara, Y. Itikawa, H. Nishimura, and M. Yoshino, J. Phys. Chem. Ref. Data **19**, 617 (1990).
[30] C. Godet, N. Layadi, and P. Roca i Cabaroccas, Appl. Phys. Lett. **66**, 3146 (1995).
[31] E. Gogolides, D. Mary, A. Rhallabi, and G. Turban, Jpn. J. Appl. Phys., Part 1 **34**, 261 (1995).
[32] M. Capitteli, G. Collona, K. Hassouni, and A. Giquel, Plasma Chem. Plasma Process. **16**, 153 (1996).
[33] S. Stamou, E. Amanatides, and D. Mataras, High Temp. Mat. Processes **3**, 255 (1999).
[34] H. Chatham, D. Hills, R. Robertson, and A. Gallagher, J. Chem. Phys. **81**, 1770 (1984).
[35] S. Tsurubuchi, K. Motohashi, S. Matsuoka, and T. Arikawa, Chem. Phys. **161**, 493 (1992).
[36] A. V. Phelps, J. Phys. Chem. Ref. Data **19**, 653 (1990).
[37] E. Amanatides, S. Stamou, S. Bogoshian, and D. Mataras, in Proceedings of 16th European Photovoltaic Solar Energy Conference, Glasgow, 2001, Vol. I, p. 581.
[38] J. Perrin and J. P. M. Schmitt, Chem. Phys. **67**, 167 (1982).
[39] J. Abrefah and D. R. Olander, Surf. Sci. **209**, 291 (1989).
[40] E. Srinivasan and G. N. Parson, J. Appl. Phys. **81**, 2847 (1997).
[41] A. Matsuda, Thin Solid Films **337**, 1 (1999).
[42] A. Matsuda and T. Goto, Mater. Res. Soc. Symp. Proc. **164**, 3 (1990).
[43] J. Perrin, M. Shiratani, P. Kae-Nune, H. Videlot, J. Jolly, and J. Guillon, J. Vac. Sci. Technol. A **16**, 278 (1998).
[44] M. Hertl and J. Jolly, J. Phys. D **33**, 381 (2000).
[45] J. M. Jasinski and J. O. Chu, J. Chem. Phys. **88**, 1678 (1988).
[46] E. Amanatides, D. Mataras, and D. E. Rapakoulias, High Temp. Mat. Processes **4**, 563 (2000).
[47] M. Kondo, M. Fukawa, L. Guo, and A. Matsuda, J. Non-Cryst. Solids **266–269**, 84 (2000).
[48] E. Amanatides, D. Mataras, and D. E. Rapakoulias, Thin Solid Films **383**, 15 (2001).

Downloaded 06 Dec 2001 to 150.140.190.25. Redistribution subject to AIP license or copyright, see http://ojps.aip.org/japo/japcr.jsp